SPi	Journal Code				Article ID				Dispatch: 10.01.14	CE: Amasula, Jennifer Nicole
	W	E			1	7	1	0	No. of Pages: 16	ME:

WIND ENERGY
Wind Energ. (2014)
Published online in Wiley Online Library (wileyonlinelibrary.com). DOI: 10.1002/we.1710

RESEARCH ARTICLE

Soil–structure reliability of offshore wind turbine monopile foundations

Wystan Carswell[1], Sanjay Raja Arwade[1], Don J. DeGroot[1] and Matthew A. Lackner[2]

[1] Department of Civil and Environmental Engineering, University of Massachusetts—Amherst, 130 Natural Resources Road, Amherst, Massachusetts 01003, USA

[2] Department of Mechanical and Industrial Engineering, University of Massachusetts—Amherst, 160 Governors Drive, Amherst, Massachusetts 01003, USA

ABSTRACT

An overview of offshore wind turbine (OWT) foundations is presented, focusing primarily on the monopile foundation. The uncertainty in offshore soil conditions as well as random wind and wave loading is currently treated with a deterministic design procedure, though some standards allow engineers to use a probability-based approach. Laterally loaded monopile foundations are typically designed using the American Petroleum Institute *p-y* method, which is problematic for large OWT pile diameters. Probabilistic methods are used to examine the reliability of OWT pile foundations under serviceability limit states using Euler–Bernoulli beam elements in a two-dimensional pile–spring model, non-linear with respect to the soil springs. The effects of soil property variation, pile design parameters, loading and large diameters on OWT pile reliability are presented. Copyright © 2014 John Wiley & Sons, Ltd.

KEYWORDS

monopile; offshore wind turbine; reliability; soil–structure interaction

Correspondence

W. Carswell, Department of Civil and Environmental Engineering, University of Massachusetts—Amherst, 130 Natural Resources Road, Amherst, Massachusetts 01003, USA.

E-mail: carswell@ecs.umass.edu

Received 10 October 2013; Revised 30 November 2013; Accepted 13 December 2013

1. INTRODUCTION

As the search for renewable energy sources intensifies, attention has turned to offshore wind turbines (OWTs) as potentially significant contributors to global electrical generation. Placing wind energy-generating equipment offshore mitigates some impacts of onshore turbines such as visual pollution, noise and long transmission distances but exacerbates issues such as operation and maintenance costs, load magnitude, complexity and uncertainty associated with support structure design.[1] This paper describes how uncertainty in the mechanical properties of subsea soil can contribute significant uncertainty in the response of OWT monopile support structure to offshore loads.

When examining an OWT as an engineered system, the three primary sources of uncertainty for the support structure are aerodynamic loading, hydrodynamic loading and soil properties. Other sources of uncertainty such as mechanical/electrical reliability and material strength (e.g. of blade composites) affect the rotor-nacelle assembly but are less significant for the support structure. Uncertainty due to fatigue can be associated with all elements of the OWT but was not in the scope of this paper, which has as its focus the distinct role that soil property uncertainty plays in response uncertainty.

Of the primary sources affecting OWT support structures, soil properties have been least investigated in a probabilistic context but are particularly important in defining the response of monopile foundation systems (where there is minimal redundancy and the overturning moment must be completely resisted by the lateral interaction between the pile with the surrounding soil). Contributing to soil property uncertainty in the offshore environment are the high cost and logistical challenges of performing detailed soil sampling at potential turbine locations and the significant challenges present in measuring *in situ* soil properties. Thus, even when extensive site investigation has been conducted, significant uncertainty regarding soil properties can persist.

Offshore wind turbine support structure designs are chosen according to water depth, which drives the design bending moments,[2,3] cost and dynamic response. Water depths are typically separated into the categories of shallow (0–30 m), transitional (30–50 m) and deep (50–200 m). Monopile support structures are deployed in water depths up to approximately 35 m, after which the flexibility of the support tower becomes an issue.[1,4,5] The monopile design is straightforward, providing a direct load path from the tower to the soil and clearly defines the loading from wind and waves (e.g. as opposed to a tripod or trussed substructure). These features of monopile design, coupled with its current dominance in the OWT domain,[6] lead to this paper's focus on probabilistic soil–structure interaction of a monopile foundation.

The following examines OWT soil–structure interaction using probabilistic methods in an effort to progress toward a reliability-based design procedure for OWT support structures, as recommended in a report from the US National Academies.[7] Considering a sandy site typical of the North Sea, the current procedure for deterministically designing laterally loaded pile foundations is presented and discussed. Using probabilistic modeling, the sensitivity of monopile reliability with respect to a serviceability limit state and in regards to soil variability, pile design parameters and load uncertainty is demonstrated. Additionally, these results show that large pile diameter effects can significantly affect monopile reliability.

2. PROBABILISTIC METHODS IN DESIGN STANDARDS

Offshore wind turbine foundations pose an interesting design problem as they are subjected to random wind and wave loads and are situated in variable soil conditions that are difficult to characterize. Despite the amount of randomness inherent in the problem, OWT foundations are typically designed using a deterministic procedure with partial safety factors (similar to load and resistance factor design). The main OWT design standards and guidelines are Det Norske Veritas (DNV), Germanischer Lloyd, International Electrotechnical Commission (IEC) and most recently, American Bureau of Shipping. With the exception of IEC (which does not directly discuss reliability-based structural design), all guidelines indicate that probabilistic methods may be appropriate for the design of novel and special cases.[8–11] In addition to this, DNV allows probabilistic analysis as a way of calibrating partial safety factors.[9] If probabilistic methods are used, the guidelines do not provide further guidance and generally require special permissions.

The design guidelines separate limit states for OWTs into two main categories: ultimate limit state (ULS) and serviceability limit state (SLS). ULSs describe the destructive failure of the OWT (such as yield or buckling), whereas SLSs refer to the limiting conditions under which the OWT can continue operating effectively. Several researchers have used probabilistic methods to analyse OWTs, but the majority of these researchers were concerned with ULS and fatigue limit states and also more with loading uncertainty than geotechnical uncertainty.[12–14]

The research presented here uses SLS and considers the effect of variable soil properties and random loading on OWT foundation reliability. SLS for monopiles are defined by specific mudline displacement and rotation limits that occur before pile ULS are reached and consequently are expected to be more sensitive to soil properties than the ULS of the support structure. While fatigue is often a design driver for monopiles, the 50 year events considered in this paper are assumed to be of short duration. The focus here is therefore primarily on analysis of the soil–pile system under peak static loads. Some recent design standards have considered the low-cycle fatigue accumulations from a short-duration extreme event to dominate pile behavior (with respect to accumulated pile head rotations) as opposed to long-term cyclic loading.

3. API *P-Y* METHOD FOR SANDS

All design standards recommend the American Petroleum Institute (API) *p-y* method for designing pile foundations, which models soil–pile resistance using a series of non-linear springs along the length of the pile.[15] The deflection of a certain soil spring at position x below the mudline is denoted by y. Based upon Winkler Foundation theory, the soil–pile resistance p (in units of force per length) for sands is defined by

$$p = Ap_u \tanh\left(\frac{kx}{Ap_u}y\right) \tag{1}$$

where

$$A = \begin{cases} \left(3 - 0.8\dfrac{x}{b}\right) \geq 0.9 \text{ for static loading} \\ 0.9 \text{ for cyclic loading} \end{cases} \tag{2}$$

and

$$p_u = \min\begin{cases} (C_1 x + C_2 b)\gamma' x \\ C_3 b \gamma' x \end{cases} \quad (3)$$

where C_1, C_2 and C_3 are coefficients, k is the modulus of subgrade reaction determined as a function of φ' (friction angle of the soil) using correlations provided by API, b is the diameter of the pile and γ' is the submerged unit weight of the soil.

The API method for determining *p-y* curves was based on testing of slender piles of 0.6 m diameter and confirmed for pile diameters up to 2 m[16]; however, monopiles with diameters up to 4.5 m have been designed using this method and subsequently installed. Using the API *p*-y method for large-diameter piles can lead to overestimation of pile–soil stiffness,[17,18] which is attributed to a combination of soil stiffness overestimation at large depths and the very large bending stiffness typical of large diameter piles. The large bending stiffness is thought to be a factor because the smaller, more flexible piles used in calibrating API *p-y* curves behave as slender beam columns, and large diameter monopiles may behave closer to beam columns in which the lateral behavior is dominated by shear deformations.[19]

The API method applies a factor of 0.9 to *p-y* curves for cyclic conditions which, although based on theoretical considerations, was determined empirically.[20] There is some evidence that this factor is appropriate only for relatively low cycle counts (e.g. 200 cycles) rather than the much larger number of loading cycles that may occur over the design lifetime of the system.[21] Since current thought is that low-cycle soil–pile fatigue during discrete storm events dominates soil–pile behavior, it is appropriate that this factor may be consistent with low cycle conditions.

Despite the shortcomings of the API *p-y* method, it is unanimously recommended by design guidelines and standards for laterally loaded piles. The goal of the analysis here is not to evaluate the appropriateness of the API method in the context of OWTs but to provide information on the uncertainty (primarily with respect to soil) produced by deterministic design.

4. REFERENCE PILE AND MODEL DEVELOPMENT

The properties of the reference pile (Table I) are taken from a pile foundation designed by Lesny, Paikowsky and Gurbuz[18] for a 5 MW OWT in the German part of the North Sea. **T1**

Quasistatic mudline loads, which are consistent with IEC design load case 6.1c, were applied to the pile head (Table II), modeling 50 year extreme wave events with reduced 50 year wind gust and standby operating conditions for the OWT.[11,22] **T2**

As part of the pile–spring model developed for this study, the pile and soil spring geometry were defined by nodal coordinates. From these coordinates, Euler–Bernoulli beam elements representing the pile were further defined by cross-sectional area, moment of inertia and modulus of elasticity. The reference pile is supported laterally by soil springs and vertically by a roller. When combined with applied mudline loads (Table II) and support conditions, the quasistatic analysis—non-linear in the response of the soil springs—provided the full set of nodal displacements (Figure 1). **F1**

The non-linear stiffness of the soil spring elements was defined according to the API *p-y* method using the non-cohesive soil properties in Table III.[22] Although these soil properties are not site-specific, they are consistent with the pile design and loading representative of typical sites in the North Sea. **T3**

Soil non-linearity was accounted for by using a simple-step load-controlled incremental solution with the soil spring tangent stiffness calculated at each step. This tangent stiffness k_t is taken from the derivative of the *p-y* curve (Equation 1) with respect to y and multiplied by the tributary length of the spring (x_k),

Table I. Properties of reference model pile foundation.

Symbol	Property	Value
b	Pile diameter	6 m
d	Pile depth	38.9 m
t	Wall thickness	0.07 m
E	Modulus of elasticity	200 GPa

Table II. Loads applied to the pile head of the reference model.

Symbol	Property	Value
V	Axial load	35 MN
H	Horizontal load	16 MN
M	Moment	562 MN-m

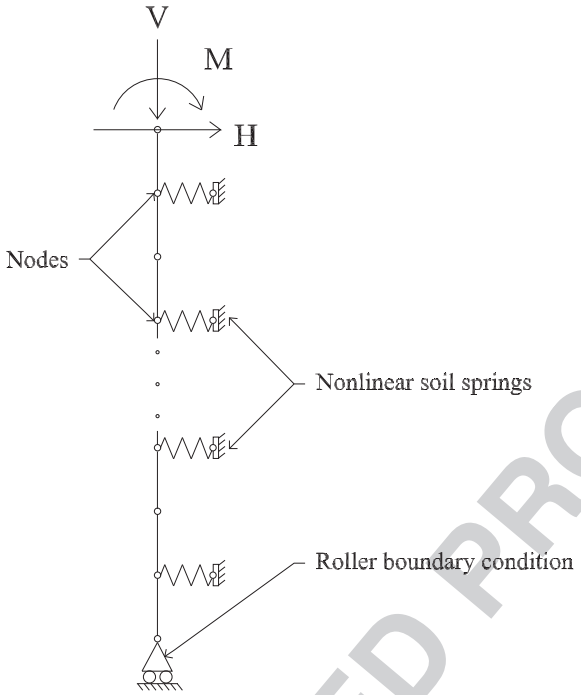

Figure 1. Example model with mudline loads applied.

Table III. Soil properties for reference model.

Symbol	Property	Value
γ'	Submerged unit weight	10 kN m^{-3}
D_R	Relative density	0.55
k	Initial modulus of subgrade reaction	19,000 kN m^{-3}
φ'	Friction angle	40.5°

$$k_t = x_k \frac{dp}{dy} = x_k \left(-kx \left(tanh^2 \frac{kxy}{Ap_u} - 1 \right) \right) \tag{4}$$

where y is the compression of the spring at the start of the current solution step. This tangent stiffness therefore represents the stiffness of the soil spring at a particular displacement y, determined by the incremental load applied in the previous steps.

The finite element model was validated by analysing the design capacity load case in which only a mudline moment of 855 MN-m was applied to the pile (with $V = H = 0$).[18] This load was chosen for validation since it is higher than the load applied to assess soil–pile reliability and drove the soil springs farther into the non-linear response range, therefore exercising the analysis code more thoroughly. The developed model (using 20 soil springs and 40 elements evenly distributed along the depth of the pile) predicted a displacement of 0.104 m, which differs from the reported displacement of 0.109 m[18] by approximately 5%.

A deterministic relationship was assumed between the soil properties, relative density D_R and friction angle φ' because parameters k and p_u in Equation 4 as defined in the American Petroleum Institute [15] depend variously on φ' and D_R. By assuming a relationship between φ' and D_R, all soil property parameters of the non-linear soil–pile stiffness (Equation 4) can be expressed as functions of the single parameter, φ'. API implies the relationship between φ' and D_R by defining k as a function of either φ' or D_R (Table IV).[15] By adopting this implied relationship and assuming γ' to be constant, the non-linear soil–pile stiffness can be determined as a function of only one soil parameter, φ'. **T4**

The reference soil is a medium dense to dense sand[18]; consequently, in order to draw a deterministic relationship between φ' and D_R, the relationship implied by API in Table IV was plotted in Figure 2 for φ' in the range of medium dense to dense sands (30° to 40°). **F2**

Table IV. Density classification of sands.

Relative density	Density classification	Friction angle
<20%	Very loose	28–29°
20–40%	Loose	29–30°
40–60%	Medium dense	30–36°
60–80%	Dense	36–40°
80%<	Very dense	40–45°

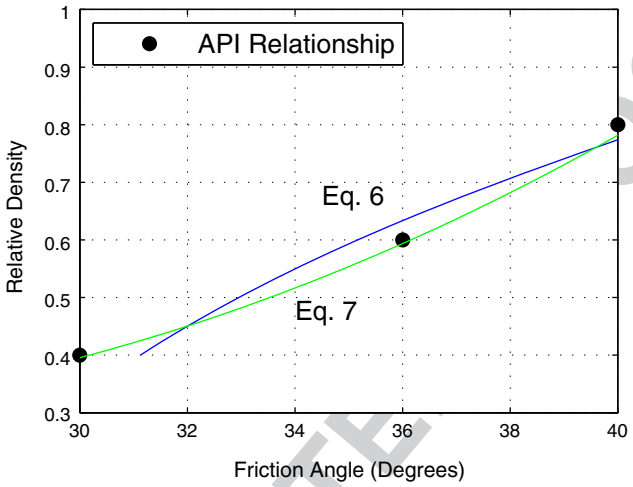

Figure 2. Relative density versus friction angle for dense to medium dense sands.

Several authors have proposed a relationship between φ' and D_R such as that of Rankine *et al.*[23] for coarse grained hydraulic fills in Australia with $D_R > 35\%$:

$$\varphi' = 19D_R^2 + 33 \tag{5}$$

Using the form of Equation 5, Equation 6 is a best-fit equation between φ' and D_R per API for medium dense to dense sands (Figure 2).

$$\varphi' = 20.2D_R^2 + 27.9 \tag{6}$$

An alternative and better fit for φ' and D_R according to the implied API relationship is the second-order polynomial

$$D_R = 0.0014\ \varphi'^2 - 0.0594\ \varphi' + 0.918 \tag{7}$$

The polynomial in Equation 7 was used in the proceeding analyses to estimate D_R as a function of φ'. This relationship altered the soil spring stiffness, reducing the predicted lateral displacement to 0.101 m (as compared with the 0.109 m reported[18]).

5. SOIL PROPERTY UNCERTAINTY MODELS

Soil property uncertainty generally results from a lack of knowledge or information rather than inherent randomness, however, modeling soil property variability with random variables and processes to facilitate modeling and greatly assist engineers in using geotechnical data for design.

The normal, or Gaussian, probability distribution is commonly used to model variability in soil properties partially because it simplifies calculations. Non-Gaussian distributions are also useful, as many soil properties are bounded by particular ranges (i.e. non-negative values) or are skewed. Typically, lognormal distributions are used for soil properties with lower bounds; however, the DNV also recommends the beta distribution for soil properties lower and upper bounds and for which the mean and standard deviation are known.[24] The beta distribution model for φ' was selected because of the

flexibility of distribution shape, permitting an analysis which examined various distribution skews which the lognormal distribution is incapable of. Friction angle was assumed to be bounded by the medium dense to dense range $30° < \varphi' < 40°$, corresponding to φ' that commonly occur in subsea sands, where

$$\varphi' = a_1 f + a_2 \tag{8}$$

$$f(\varphi';A,B) = (Beta(A,B))^{-1}\varphi'^{A-1}(\varphi' - 1)^{B-1} \tag{9}$$

where a_1 is the range of φ' considered, a_2 is the minimum bound of φ', A and B are distribution parameters and *Beta* is the beta function.

Because of the variability of soil properties from site to site (and within a site), Baecher and Christian caution that it is neither 'easy nor wise to apply typical values of soil property variability… for a reliability analysis'.[25] For realistic pile design or reliability calculation, site-specific geotechnical data is a necessity. Trends are fit to the data, likely characterized using an autocovariance or autocorrelation function and pile design proceeds based upon the findings of this type of data analysis. Without a detailed site investigation from the North Sea site, no conclusive design decisions can be made from the proceeding analyses. The results presented here establish sensitivity of OWT support structure reliability with respect to soil property distribution and pile design parameters, as well as comparing the propagation of uncertainty from soil and load variability.

Phoon[26] and Baecher and Christian[25] proposed coefficient of variation (COV) ranges for φ' as listed in Table V. **T5**

Lacasse and Nadim[27] report the COV in φ' for sands (on the basis of laboratory tests) to be between 2–5%. Higher COV values have been reported (e.g. 30% by Sett and Jeremić[28]), but such observations often include various measurement methods and consider sands and clays together. Because the analysis presented in this paper focuses on soil–structure interaction in sands, 5% COV for sands was the maximum considered COV.

Spatial correlation in soil properties is somewhat dependent on soil type and testing method and is extremely site-dependent.[29] A probabilistic model for soil properties should be able to capture the distribution of the soil properties and spatial variation as quantified by the spatial autocorrelation function. The non-Gaussian φ' is in turn modeled using a translation model that allows matching of a target marginal distribution and spatial correlation function

Table V. COV ranges for friction angle.

Property variability	COV (%)
Low	5–10
Medium	10–15
High	15–20

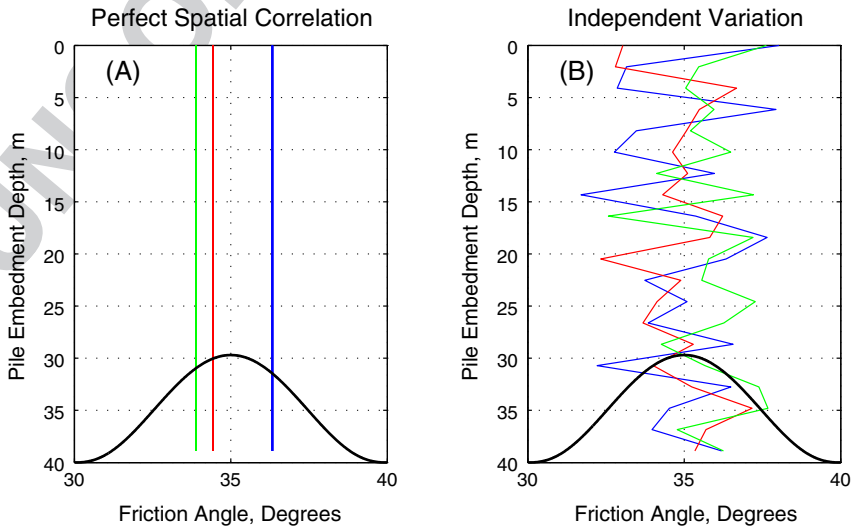

Figure 3. Sample realizations of random soil profiles in terms of friction angle. (a) Soil profile with perfect spatial correlation where a single random friction angle is defined for the entire depth of the pile. (b) Soil profile with the friction angle at each soil spring is independent of other soil springs. In both cases, the bold curve at the bottom defines the marginal beta distribution of the friction angle.

Colour online, B&W in print

Wind Energ. (2014) © 2014 John Wiley & Sons, Ltd.
DOI: 10.1002/we

$$\varphi'(x) \sim \left(F_{\varphi'}(\varphi'), C_{\varphi'\varphi'}(|x_1 - x_2|)\right) \tag{10}$$

where $F_{\varphi'}$ is the cumulative distribution function representing φ', $C_{\varphi'\varphi'}$ is the covariance function and x_1 and x_2 are two points along the length of the pile.

In the absence of data from a specific site investigation to develop an autocovariance function for φ', this study considered two limiting cases: perfect correlation (infinite correlation length) and independent variation (zero correlation length). In terms of Equation 10, independent variation corresponds to $C_{\varphi'\varphi'}(|x_1 - x_2|) = \delta(|x_1 - x_2|)$, where $\delta(|x_1 - x_2|)$ is the Dirac delta function, and perfect correlation corresponds to $C_{\varphi'\varphi'}(|x_1 - x_2|) = \sigma^2_{\varphi'}$, the variance of φ'.

In the case of perfectly correlated soil conditions, the soil properties for the complete depth of the pile are defined by a single random sample drawn from the distribution of φ'. For independent spatial variation, φ' is sampled independently from the same model distribution for each of the soil springs (Figure 3). It is important to note that although the distribution **F3** of φ' is assumed to be constant with depth, the resulting soil mechanical properties such as elastic modulus and strength, as embodied in the *p-y* curves, vary with depth because of the dependence of the *p-y* curve formulation on depth.

Figure 3 compares three sample realizations of φ' from the same target distribution (shown in both cases as the bold curve at the bottom), considering perfect spatial correlation and independent variation.

Although model uncertainty certainly plays a role in the total uncertainty of predictions of soil–pile response, this paper focuses only on the soil property uncertainty itself. Investigation of model uncertainty represents an entirely different research question, and the adoption of industry standard models here (*p-y* curves) allows the soil property uncertainty analysis to be placed in the context of widely accepted models. The uncertainties reported here, therefore, represent lower bounds on the total uncertainty, which would include model uncertainty.

6. RELIABILITY ANALYSIS METHOD

A first-order second moment reliability method (FOSM) and Monte Carlo simulation (MCS) was used to estimate the reliability of the reference pile. The reliability index (β) is often used to concisely express small probabilities of failure with the probability of failure (P_f) calculated from β by

$$P_f = \Phi(-\beta) \tag{11}$$

where Φ is the standard normal cumulative distribution function. An estimation of β can be made from the mean and standard deviation of the limit state safety margin with the assumption that the pile response is Gaussian. OWTs are designed for a target safety level equivalent to an annual $P_f = 10^{-4}$, which corresponds to $\beta = 3.7$[9]

Serviceability limit state for OWT pile foundations can restrict horizontal pile head rotation (α) to 0.7°.[16] Using these criteria to establish the safety margin yields

$$g(\alpha) = 0.7 - \alpha \tag{12}$$

where $g(\alpha)$ is the safety margin and in which α depends on the loading, pile bending stiffness and soil–pile resistance. The safety margin is defined such that $g < 0$ indicates a violation of the limit state. The second moment properties (mean μ_g, standard deviation σ_g) of the safety margin can be estimated via MCS, and the reliability index (β) is then calculated as

$$\beta = \frac{\mu_g}{\sigma} \tag{13}$$

7. RESULTS

Parametric studies were conducted to observe the effect of soil property correlation, soil property variation, pile bending stiffness, embedment depth and load variation on OWT monopile reliability. A total of 10,000 MCS were run to estimate the mean and standard deviation of the safety margin yielding accuracy of ±0.1 in the estimate of β.

Treating the quasistatic loads from Table III as deterministic and focusing on the effects of soil variability alone, perfectly correlated $\boldsymbol{\varphi}'$ defined by a beta distribution with $\mu_{\varphi'} = 35°$ and 5% COV produced $\beta = 3.8$ (Table VI). **T6**

It should be noted that in this case, β only takes into account the uncertainty with respect to soil property variation and is therefore higher than what may be expected with further consideration of uncertainty.

Table VI. Comparison of reliability results from correlation limiting cases.

Correlation length	μ_α	σ_α	μ_g	σ_g	β	P_f
0	0.576°	0.027°	0.124°	0.027°	4.6	2.1×10^{-6}
∞	0.575°	0.033°	0.125°	0.033°	3.8	7.2×10^{-5}

7.1. Correlation

Using the same beta distribution, the effect of spatial correlation on $g(u, \alpha)$ was taken into account by comparing the results from perfectly correlated soil properties versus independently varying soil properties (Table VI).

Whereas both analyses yielded approximately the same mean α, the standard deviation α was higher for the perfectly correlated case than for independent variation. Figure 4 illustrates the wider spread of rotations experienced by the pile head when φ' variation is modeled with perfect correlation. **F4**

The lesser variability of α for the independent variation case can be understood by considering α to be approximately a function of the average φ' along the depth of the pile. Since in the perfect correlation case φ' is constant with depth but varies between samples, the sample-to-sample variation of the average φ' is greater in the perfect correlation case than for the independent variation. This observation emphasizes the importance of φ' with respect to soil–pile stiffness in the *p-y* method.

Figure 5 shows α on the basis of depth-averaged φ' (for independently varying soil properties). The best-fit linear regression shows the expected inverse relationship between average φ' and α, but the significant scatter shows that the average of φ' is not sufficient to characterize soil–structure interaction. **F5**

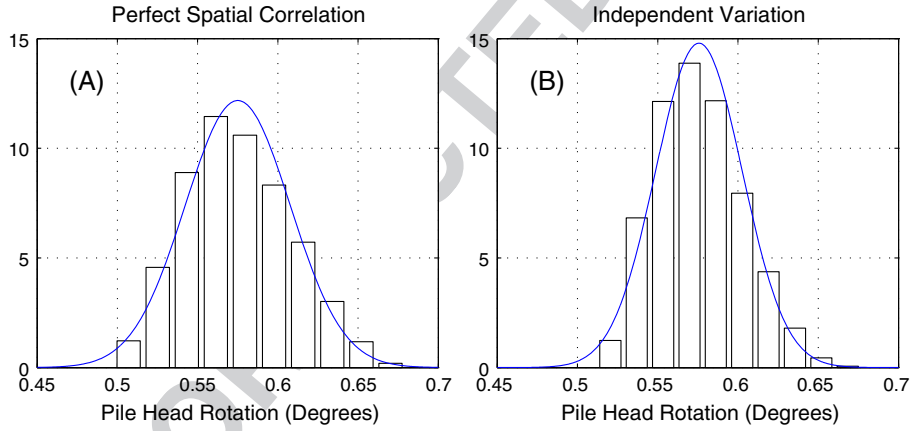

Figure 4. Comparison of pile head rotation and Gaussian probability density function.

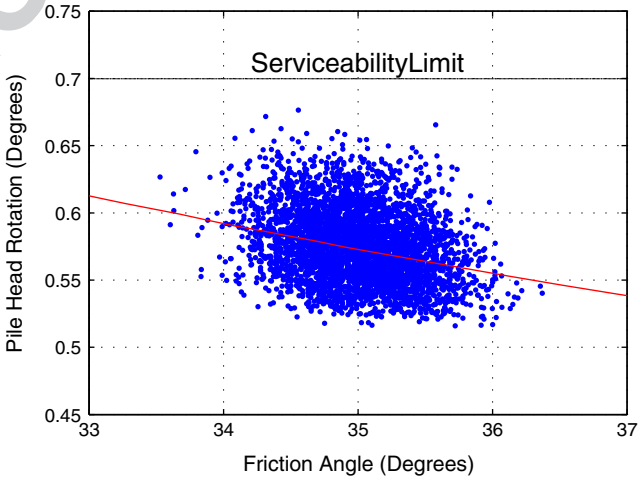

Figure 5. Pile head rotation versus average friction angle.

Wind Energ. (2014) © 2014 John Wiley & Sons, Ltd.
DOI: 10.1002/we

It is evident for the limiting cases of independent variation and perfect correlation that soil property correlation plays a significant role in reliability analysis (Table VI); both limiting cases are presented in this paper to gauge the potential range of β. Q1

The spatial discretization of the pile springs (approximately one spring per 2 m of pile) implicitly assumes a correlation of soil properties with depth; however, an analysis with twice the number of soils springs (40 in total, approximately one spring per meter of pile) and independently varying φ' also yielded a reliability index of 4.6. This result demonstrates that further discretization beyond one spring per meter does not significantly influence SLS reliability and that 20 springs are sufficient for modeling independently varying soil properties with depth.

Despite the symmetry of the φ' distribution, the distribution of α is mildly skewed due to the non-linearity of mapping φ' to α (this mild skewness can be seen by comparing the histograms of alpha in Figure 4 with the overlaid best-fit Gaussian distributions). Non-Gaussianity of α introduces some degree of error into the FOSM estimate of reliability; although this error could be avoided by estimating reliability through direct MCS, such an approach is only practical when the reliability is significantly lower than observed herein.

To quantify the error introduced to the estimates of β by non-Gaussianity of α, reliabilities have been estimated in a limited number of cases using an alternative approach. In that approach, a lognormal distribution [$F_{\alpha,lognormal}(\alpha)$] is fit to the MCS of α, and an alternative estimate of the reliability index can be determined by

$$\beta = \Phi^{-1}\left(1 - F_{\alpha,lognormal}(0.7^\circ)\right) \tag{14}$$

Table VII demonstrates that whereas the lognormal estimates of β are slightly lower than the Gaussian estimates, the reliabilities are similar, and differences in magnitude between zero and infinite correlation length as well as a φ' COV of 5% to 8.25% are comparable. Given that the FOSM estimates of β correctly capture trends in reliability and do not differ greatly from those obtained by fitting a lognormal distribution, the FOSM estimates of β are used in the remainder of this paper. This choice is made both to simplify the analysis and because accurately fitting the upper tail of the distribution of α would not be possible without a significant increase in MCS. T7

The non-Gaussianity of α should be acknowledged; however, the goal of this paper is to analyse sensitivity of SLS reliability for monopiles; therefore, the primary focus is on differences in β and not the precise value of β. As aforementioned, uncertainty due to loading and non-geotechnical material properties has not been considered in these reliability estimations.

7.2. Friction angle variance

The effect of φ'variance on β was examined using a range of symmetric beta distributions with $\mu_{\varphi'} = 35^\circ$ (Table VIII). This range was selected on the basis of the minimum COV of 2% from Lacasse and Nadim[26] and the maximum COV 8.25% corresponding to a uniform distribution (equal probability of any value of φ' occurring, where $A = B = 1$). T8

Table VII. Reliability indices assuming a lognormal and gaussian distribution.

		β, Lognormal		β, Gaussian	
	Correlation length	0	∞	0	∞
COV	5%	4.2	3.5	4.6	3.8
	8.25% (uniform)	2.4	2.0	2.6	2.2

Table VIII. Beta distribution parameters for examining the effect of friction angle variance on reliability.

μ (°)	σ (°)	COV (%)	A	B
35.0	0.700	2.00	25.00	25.00
35.0	1.05	3.00	10.83	10.83
35.0	1.40	4.00	5.875	5.875
35.0	1.75	5.00	3.577	3.577
35.0	2.10	6.00	2.334	2.334
35.0	2.45	7.00	1.587	1.587
35.0	2.80	8.00	1.095	1.095
35.0	2.89	8.25	1.000	1.000

By plotting β against the COV of φ', it can be seen that as COV increases, β decreases non-linearly (Figure 6). It is also interesting to note that the difference between β for independent variation and perfect correlation appears to decrease slightly with increasing COV. F6

Specifications for OWT foundations do not explicitly define a target reliability index with respect to SLS. Therefore, the 50 year SLS target reliability index of $\beta = 1.5$ that is specified for Consequence Class 2 structures in Eurocode[30] is adopted as a reference SLS reliability for comparison purposes in this study. The reliability indices for all the cases shown in Figure 6 exceed the reference SLS target reliability index of $\beta = 1.5$. This is likely an indication that the design of the pile referenced in the work by Lesny *et al.*[18] was not controlled by SLS reliability but rather by ULS (i.e. strength) reliability, stiffness or the need to ensure sufficient fixity of the pile tip. Nevertheless, the results give a clear indication of the non-linear sensitivity of the SLS reliability index to the magnitude of the uncertainty in φ'.

7.3. Friction angle distribution shape

One of the main benefits of a beta distribution is its flexibility, both in distribution shape and because it can be bounded above and below. This paper focuses on a particular range of φ' values (30–40°), but there are an infinite number of possibilities for the shape of the beta distributions representing φ'. Changing the shape of the distribution changes both the mean and variance of φ'. The range of beta distribution parameters considered in this section (Table IX, $1 < A,\ B < 3.577$) T9 corresponds to the range between a uniform distribution ($A = B = 1$) and symmetric 5% COV beta distribution ($A = B = 3.577$). Symmetric distributions can be seen on the diagonal, where the parameters $A = B$ ($\mu_{\varphi'} = 35°$). The values used for A and B were evenly spaced along the interval 1 to 3.577, with several example distributions can be seen in Figure 7. F7

Table X shows the resulting values of β from the φ' distributions in Table IX. Perfectly correlated case results were T10 shown because this assumption results in higher probabilities of failure (lower β), and the effect of spatial correlation on β was relatively consistent across all quasistatic cases examined.

Reliability index rises from 2.2 to 6.0 when B is 1 and A varies from 1 to 3.557. The dramatic change and high reliability indices can be attributed to the somewhat unrealistic φ' distributions in Figure 7(b), which show a high concentration of

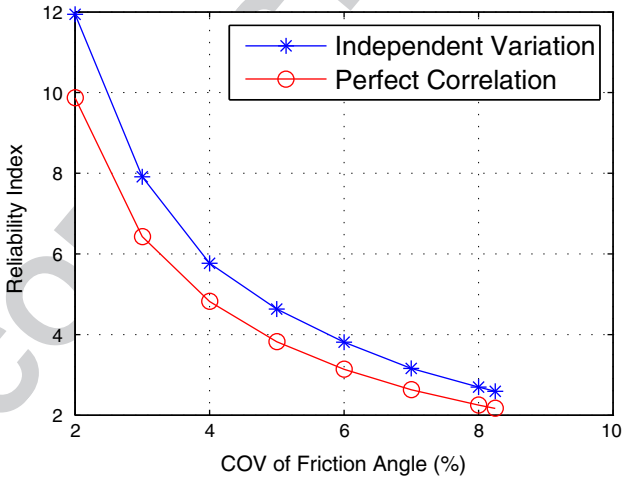

Figure 6. Reliability index versus COV of friction angle.

Colour online, B&W in print

Table IX. Mean and standard deviation (μ, σ) of friction angle with respect to beta parameters (A, B).

	B					
A	1.000	1.515	2.031	2.546	3.062	3.5770
1.000	35.0, 2.89	34.0, 2.61	33.3, 2.34	32.8, 2.11	32.5, 1.91	32.2, 1.75
1.515	36.0, 2.61	35.0, 2.49	34.3, 2.32	33.7, 2.15	33.3, 1.99	33.0, 1.85
2.031	36.7, 2.34	35.7, 2.32	35.0, 2.22	34.4, 2.10	34.0, 1.98	33.6, 1.87
2.546	37.2, 2.11	36.3, 2.15	35.6, 2.10	35.0, 2.03	34.5, 1.94	34.2, 1.85
3.062	37.5, 1.91	36.7, 1.99	36.0, 1.99	35.5, 1.94	35.0, 1.87	34.6, 1.81
3.577	37.8, 1.75	37.0, 1.85	36.4, 1.87	35.8, 1.85	35.4, 1.80	35.0, 1.75

Wind Energ. (2014) © 2014 John Wiley & Sons, Ltd.
DOI: 10.1002/we

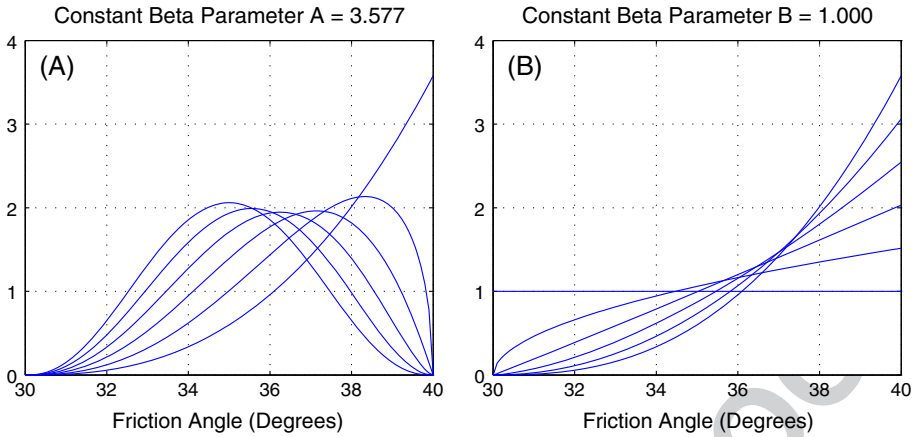

Colour online, B&W in print

Figure 7. Beta probability density functions demonstrating distribution shape flexibility (a) beta distributions with constant parameter A = 3.577. (b) Beta distributions with constant parameter B = 1.

Table X. Reliability index with respect to beta parameters, assuming perfectly correlated soil properties.

	B					
A	1.000	1.515	2.031	2.546	3.062	3.5770
1.000	2.2	1.9	1.8	1.7	1.7	1.6
1.515	3.0	2.6	2.4	2.3	2.2	2.1
2.031	3.7	3.2	3.0	2.8	2.6	2.5
2.546	4.4	3.9	3.5	3.3	3.1	3.0
3.062	5.2	4.5	4.0	3.7	3.5	3.4
3.577	6.0	5.1	4.5	4.2	4.0	3.8

probability mass near $\varphi' = 40^{o}$, corresponding to stronger soil–pile resistance. The more realistic distributions in Figure 7(a), which have a peak probability mass at a value other than $\varphi' = 40^{o}$ show a less rapid decrease of β when B increases with constant A. At the maximum considered value of A (3.577), the change in β is from 6 to 3.8. It can be concluded that reliability is more sensitive to changes in φ' distribution shapes that result in monotonic increase of the probability mass with a peak at $\varphi' = 40^{o}$.

As mentioned, some of the distributions in Figure 7 are not realistic in part because the COV of many of the distributions exceeds the maximum expected value of 5%. Considering this limit, beta probability density functions with 5% COV were Q2 selected to demonstrate more precisely how distribution behavior changes with the selection of A and B (three of these can be seen in Table XI and Figure 8). T11 F8

As A increases (and B decreases), $\mu_{\varphi'}$ shifts right. Plotting β against $\mu_{\varphi'}$, Figure 9 shows that β increases linearly with F9 constant COV.

7.4. Pile design parameters

In realistic design scenarios, pile properties are selected on the basis of the results of a site investigation. The effect of pile property selection on reliability was examined considering pile diameter, wall thickness and embedment depth with symmetric beta distribution $\mu_{\varphi'} = 35°$ and 5% COV used to model φ'.

Table XI. Beta parameters yielding approximately 5% COV.

μ (°)	σ (°)	COV (%)	*A*	*B*
31.9	1.60	4.99	1.000	4.149
32.5	1.62	5.00	1.500	4.560
33.0	1.65	5.00	2.000	4.700
33.5	1.68	5.00	2.500	4.610
34.1	1.70	4.99	3.000	4.345
35.0	1.75	5.00	3.577	3.577
36.6	1.83	5.00	3.750	1.920

Colour online, B&W in print

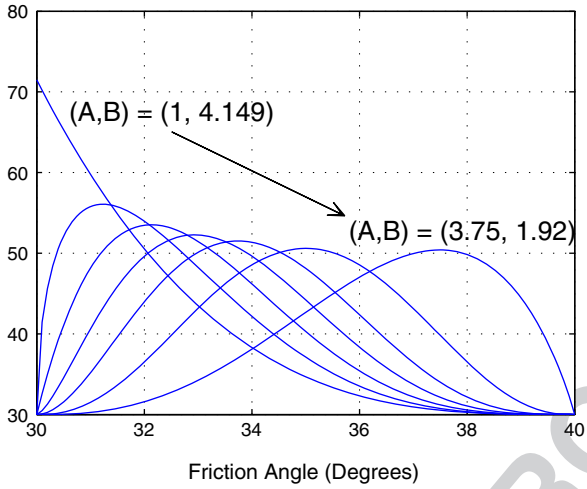

Figure 8. Beta probability density functions with approximately 5% COV.

Colour online, B&W in print

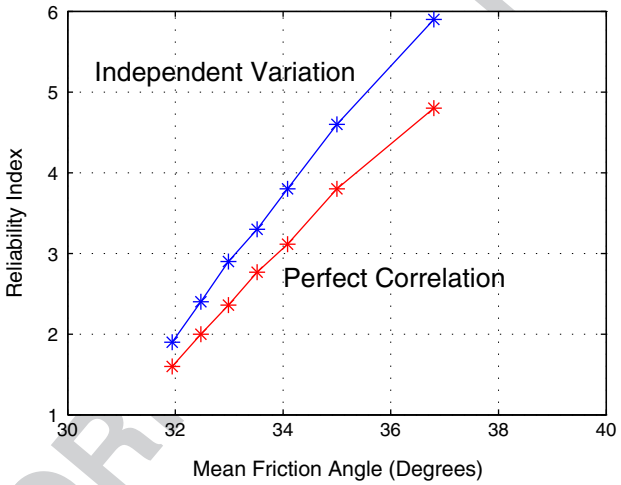

Figure 9. Reliability index versus mean friction angle for 5% COV distributions.

Figure 10 shows contour lines for the moment of inertia and SLS reliability on axes defining the pile cross section design space (thickness and diameter). The API *p-y* curves depend explicitly on the pile diameter, but the reliability contours of Figure 10 demonstrate that this diameter effect is extremely small for any thickness and diameter at a fixed moment of inertia. Investigating a greater range of pile diameters (4–7 m) than those shown in Figure 10 found the relationship between moment of inertia and reliability to be consistent. These results were not presented because the resulting SLS reliabilities are unrealistically low (in some cases negative) since the load magnitude and embedment depth remained constant for all cases. **F10**

As the wall thickness increases for fixed pile diameter (or vice versa), β increases. The increase is faster when the pile diameter is increased with fixed wall thickness since the pile moment of inertia depends on the cube of the radius. In terms of the design of monopile foundations, it is more instructive to note that the moment of inertia and reliability contours are essentially parallel to one another; this implies that to reach a target SLS reliability (with all other system parameters fixed), the designer can choose any combination of pile diameter and wall thickness that achieves the appropriate moment of inertia. For example, a designer may want to increase wall thickness to mitigate against buckling, but must be cognizant of the challenges of working with thick steel plate that would form the walls of such a pile. A contour plot assuming independently varying soil properties led to the same conclusion.

The effect of embedment depth on reliability was also analysed using the pile cross-section properties from Table I. The distance between soil springs (x_k) was held approximately constant at 1.95 m for the range of embedment depths considered (30–45 m). As embedment depth increased, β converged around 37 m of embedment with less than 1% increase in β from 37–45 m (Figure 11). This result is particularly interesting since the design was made without respect to the SLS reliability **F11**

Wind Energ. (2014) © 2014 John Wiley & Sons, Ltd.
DOI: 10.1002/we

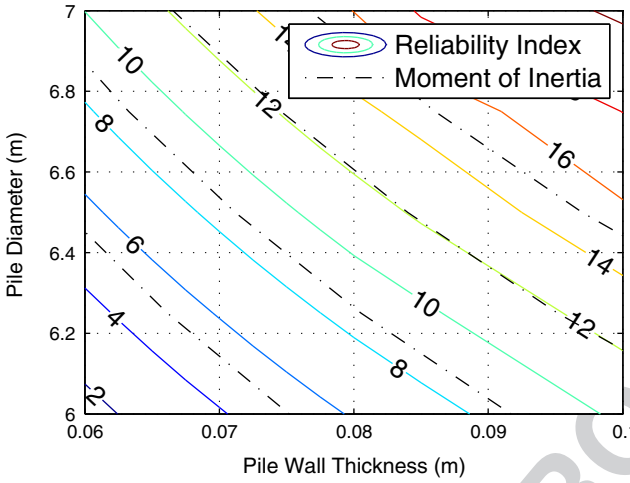

Figure 10. Contours of reliability and moment of inertia assuming perfectly correlated soil properties.

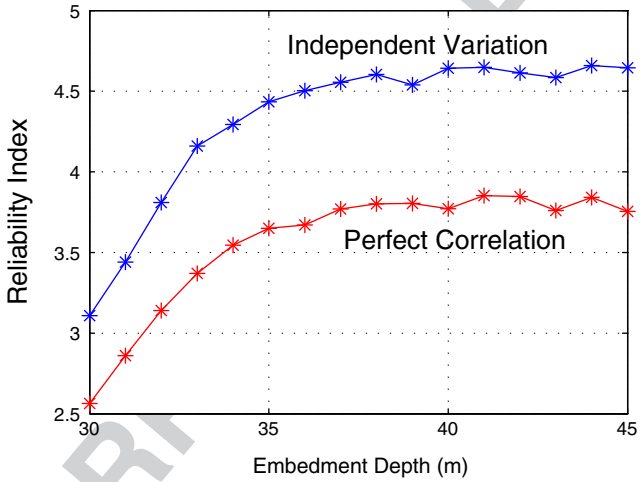

Figure 11. Reliability index as a function of embedment depth.

of the system but rather with respect to the deterministic deflections and capacities. The SLS reliability index β remains relatively constant because the flexible pile (defined by the API *p-y* method) has become essentially fully fixed; increasing embedment depth beyond this point no longer affects pile behavior.

7.5. Load variation

For the design of an OWT monopile, the applied horizontal mudline load H and overturning moment M would be calculated from site-specific data of wind and wave distributions, usually selecting loads corresponding to wind and wave events associated with a specific return period. It must be recognized, however, that estimates of these load values are themselves uncertain.

In order to investigate the relative importance of load and soil property uncertainty in defining the SLS reliability of the pile, a comparative study of load and soil uncertainty propagation was conducted.

Weibull distributions are commonly used to model probability density functions for long-term wind data. The 50 year return period load values H and M (Table III) were defined as the mean of Weibull distributions, assumed to be fully correlated and varying with a COV of 5%.

The results in Table XII demonstrate that the reliability indices that result from load and soil uncertainty are broadly similar ($\beta \approx 4$), indicating that similar amounts of uncertainty in soil and load propagate an equivalent amount of uncertainty. The SLS reliability of the pile is somewhat more sensitive to soil property uncertainty if the soil properties are perfectly correlated with depth and less so if the soil properties are uncorrelated with depth. **T12**

Table XII. Reliability index results considering combinations of load and soil randomness.

		Soil			
		Independent variation		Perfect correlation	
		Random	Deterministic	Random	Deterministic
Load	Random	3.0	4.1	2.8	4.1
	Deterministic	4.6	—	3.8	—

This analysis does not rigorously take into account the effect of load variability on OWT support structure reliability; consequently, the results in Table XII represent a minimum bound for SLS reliability.

8. CONCLUSIONS

Current design standards for OWTs utilize a deterministic design procedure that applies partial safety factors to take into account randomness in wind and wave loading. This paper uses probabilistic methods to analyse OWT monopile foundations in an effort to progress toward a reliability-based design, emphasizing the effects of soil property variation on OWT reliability. Even under best practices, geotechnical site characterization is inherently uncertain, and the limited soil information typically available cannot be fully representative of the whole design site. The approach introduced in this paper can provide direct estimates of the probability of exceedence of the design mudline rotation limit rather than the binary determination of safety provided by satisfying the mandates of a design specification. Although it would be cost-prohibitive and somewhat impractical to characterize the geotechnical uncertainty and perform a reliability-based analysis such as that described here for every potential OWT site at the design stage, such an analysis could be useful to parties with greater interest in risk assessment of the site such as insurers, financiers and regulators. Furthermore, additional research could be aimed at developing realistic but conservative models for geotechnical uncertainty that would allow approximations to the reliability-based analysis presented here to be conducted with much greater efficiency.

A static two-dimensional pile–spring model of an OWT monopile foundation situated in dense to medium dense sand was created and validated against published results.[18] Epistemic randomness in soil properties was introduced by varying friction angle (φ') along the length of the pile. The limiting cases for spatial correlation of φ' (independent variation and perfect correlation) between soil springs were considered for all parametric studies. Throughout the soil–pile interaction studies, assuming perfectly correlated soil properties yielded lower reliability than assuming independently varying properties.

A first-order method was implemented to determine the reliability index (β) of the model using the serviceability limits of the pile head (in terms of displacement and rotation) to create safety margins. Rotation dominated β and the contribution of failure probability from displacement was neglected.

As the COV of a symmetric (mean friction angle $\mu_{\varphi'} = 35°$) φ' distribution increased, β decreased non-linearly. With constant COV (5%), β increased linearly with $\mu_{\varphi'}$.

Considering that pile design is typically conducted with a given set of soil properties, the effect of pile diameter, wall thickness and embedment depth on β were examined. In a parametric study, it was determined that the bending capacity of the pile directly influenced β, rendering the effect of pile diameter within API *p-y* curves negligible by comparison. β converged around an embedment depth of approximately 37 m, which agreed with the designed embedment depth of 38.9 m.

A comparison of uncertainty propagation treated quasistatic environmental loads[18] as mean values varying with a Weibull distribution and COV of 5%. Consideration of load variation decreased β further than considering soil property variation alone, but importantly, the system showed similar sensitivity to load as to soil uncertainty. These results indicate the importance of a good site investigation and detailed soil characteristics, as soil property variability contributes significantly to overall OWT reliability.

ACKNOWLEDGEMENTS

Carswell's research was supported by the Brack Class of 1960 graduate student fellowship, partially supported through grants CMMI-1234560, CMMI-1234656, and the NSF-sponsored IGERT: Offshore Wind Energy Engineering, Environmental Science, and Policy (grant number 1068864).

REFERENCES

1. Musial W, Ram B, *et al*. Large-scale Offshore Wind Power for the United States: Assessment of Opportunities and Barriers. National Renewable Energy Laboratory: Golden, Colorado, 2010.
2. ESS Group Inc. Hydrodynamic Effects on Offshore Wind Turbine Support Structures. Prepared for Cape Wind Associates, L.L.C.: Wellesley, MA, 2004.
3. de Vries WE, Krolis VD. Effects of Deep Water on Monopile Support Structures for Offshore Wind Turbines. Delft University of Technology, Duwind, Civil Engineering and Geosciences: Delft, the Netherlands, 2004.
4. Lesny K, Hinz P. Investigation of monopile behavior under cyclic lateral loading. *6th International Offshore Site Investigation and Geotechnics Conference*. London, England, 2007; 383–390.
5. Malhotra S. Supporting the winds of change. *Civil Engineering* 2010; **8**: 76–85.
6. Wilkes J, Moccia J. The European offshore wind industry key 2011 trends and statistics. European Wind Energy Association, 2012.
7. Transportation Research Board (TRB). Structural Integrity of Offshore Wind Turbines. Special Report 305, Transportation Research Board, US National Academies: Washington, DC, 2011.
8. American Bureau of Shipping (ABS). Guide for Building and Classing Offshore Wind Turbine Installations. American Bureau of Shipping: Houston, TX, 2010.
9. Det Norske Veritas (DNV). Offshore Standard DNV-OS-J101: Design of Offshore Wind Turbine Structures. Det Norske Veritas: Høvik, Norway, 2009.
10. Germanischer Lloyd (GL). Guideline for the Certification of Offshore Wind Turbines. Germanischer Lloyd WindEnergie GmbH: Uetersen, Germany, 2005.
11. IEC 61400-3. Design Requirements for Offshore Wind Turbines. International Electrotechnical Commission, 2009. Q3
12. Rangel-Ramírez JG, Sørensen JD. Probabilistic calibration of fatigue design factors for offshore wind turbine support structures. *EWEC 2010 Conference Proceedings: Europe's Premier Wind Energy Event*. European Wind Energy Association: Warszawa, Poland, 2010.
13. Rendon EA, Manuel L. Long-term loads for a monopile-supported offshore wind turbine. *Wind Energy* 2012. DOI: 10.1002/we.1569.
14. Rose S, Jaramillo P, Small MJ, Grossman I, Apt J. Quantifying the hurricane risk to offshore wind turbines. *Proceedings of the National Academy of Sciences* 2012; **109**: 3247–3252. DOI: 10.1073/pnas.1111769109.
15. American Petroleum Institute (API). Recommended Practice for Planning, Designing, and Constructing Fixed Offshore Platforms—Working Stress Design. American Petroleum Institute: Washington, D. C., 2005.
16. Wiemann J, Lesny K, Richwien W. Evaluation of pile diameter effects on soil–pile stiffness. *Dokumentation der 7th German wind energy conference DEWEK*, 2004.
17. Klinkvort RT, Leth CT, Hededal O. Centrifuge modelling of a laterally cyclic loaded pile. In Physical Modelling in Geotechnics. Taylor & Francis: London, 2010; 959–964.
18. Lesny K, Paikowsky SG, Gurbuz A. Scale effects in lateral load response of large diameter monopiles. In Contemporary Issues in Deep Foundations: Proceedings of Sessions of Geo-Denver 2007. Geotechnical Special Publication 158: Denver, CO, 2007. DOI: 10.1061/40902(221)40.
19. Achmus M, Abdel-Rahman K. Design of piles for offshore wind energy foundations with respect to horizontal loading. ISOPE-2012, The 22nd International Offshore (Ocean) and Polar Engineering Conference; Rhodes, Greece, June 17-22.
20. LeBlanc C, Houlsby GT, Byrne BW. Response of stiff piles in sand to long-term cyclic lateral loading. *Geotechnique* 2009; **60**: 79–90. DOI: 10.1680/geot.7.00196.
21. Dührkop J. Zum Einfluss von Aufweitunge nund zyklischen Lasten auf das Verformungsverhalten lateral beanspruchter Pfähle in Sand. Dissertation, Veröffentlichungen des Institutes für Geotechnik und Baubetrieb der Technischen Universtät Hamburg-Harburg, 2010 (in German).
22. Lesny K, Wiemann J. Design aspects of monopiles in German offshore wind farms. In Frontiers in Offshore Geotechnics: ISFOG 2005. Taylor & Francis Group: London, 2005; 383–389. DOI: 10.1201/NOE0415390637.ch37.
23. Rankine KJ, Sivakugan N, Cowling R. Emplaced geotechnical characteristics of hydraulic fills in a number of Australian mines. *Journal of Geotechnical and Geological Engineering* 2006; **24**: 1–14. DOI: 10.1007/s10706-004-1511-x.
24. Det Norske Veritas (DNV). Offshore Standard DNV-RP-C207: Statistical Representation of Soil Data. Det Norske Veritas: Høvik, Norway, 2012.
25. Baecher GB, Christian JB. Reliability and Statistics in Geotechnical Engineering. John Wiley & Sons: London and New York, 2003.

26. Phoon K-K. Reliability-based Design in Geotechnical Engineering: Computations and Applications. Taylor and Francis: New York, NY, 2008.
27. Lacasse S, Nadim F. Uncertainties in characterising soil properties. In Uncertainty in the Geologic Environment: From Theory to Practice. Geotechnical Special Publication No. 58, ASCE: Madison, WI, 1996; 49–75.
28. Sett K, Jeremíc B. Forward and backward probabilistic simulations in geotechnical engineering. In Contemporary Topics in In-Situ Testing, Analysis and Reliability of Foundations. Geotechnical Special Publication No. 186: Orlando, FL, 2009; 332–339. DOI: 10.1061/41022(336)43.
29. Uzielli M, Lacasse S, Nadim F, Phoon K-K. Soil Variability Analysis for Geotechnical Practice. Taylor & Francis Group: London, 2007. DOI: 10.1201/NOE0415426916.ch3.
30. Gulvanessian H, Calgaro J-A, Holicky M. Designer's Guide to EN 1990: Eurocode: Basis of Structural Design. Thomas Telford Publishing: London, 2002. DOI: 10.1680/bsd.41714.